Numerical Investigation of Aerosol Particle Transport and Deposition in Realistic Lung Airway

Mohammad S. Islam[1]*, Suvash C. Saha[1†], Emilie Sauret[1], Y.T. Gu[1], Zoran D. Ristovski[1]

[1] School of Chemistry, Physics & Mechanical Engineering
Queensland University of Technology
2 George Street, GPO Box 2434, Brisbane QLD 4001, Australia.

*Presenting author: m20.islam@qut.edu.au
†Corresponding author: suvash.saha@qut.edu.au

Abstract

Different human activities like combustion of fossil fuels, biomass burning, industrial and agricultural activities, emit a large amount of particulates into the atmosphere. As a consequence, the air we inhale contains significant amount of suspended particles, including organic and inorganic solids and liquids, as well as various microorganism, which are solely responsible for a number of pulmonary diseases. Developing a numerical model for transport and deposition of foreign particles in realistic lung geometry is very challenging due to the complex geometrical structure of the human lung. In this study, we have numerically investigated the airborne particle transport and its deposition in human lung surface. In order to obtain the appropriate results of particle transport and deposition in human lung, we have generated realistic lung geometry from the CT scan obtained from a local hospital. For a more accurate approach, we have also created a mucus layer inside the geometry, adjacent to the lung surface and added all apposite mucus layer properties to the wall surface. The Lagrangian particle tracking technique is employed by using ANSYS FLUENT solver to simulate the steady-state inspiratory flow. Various injection techniques have been introduced to release the foreign particles through the inlet of the geometry. In order to investigate the effects of particle size on deposition, numerical calculations are carried out for different sizes of particles ranging from $1\mu m$ to $10\ \mu m$. The numerical results show that particle deposition pattern is completely dependent on its initial position and in case of realistic geometry; most of the particles are deposited on the rough wall surface of the lung geometry instead of carinal region.

Keywords: Particle Transport, Particle Deposition, Realistic Lung Airway, Mucus Layer, Pollutant Particles.

1.0 Introduction

As a result of industrialization and human activities, especially in the developing countries, air pollution has significantly increased over the last and current century. . Inhalation and exhalation, either by nose or mouth, are an essential part of the human body mechanisms. During the breathing process, we inhale pollutant particulates mix with air that can cause fatal disease. In the case of inhalation, our nasal cavities and oral airways act as a filter. Most of the inhaled micron particles basically deposit in the nasal cavities and oral region during the inhalation process due to inertial impaction and strong turbulent dispersion [Feng and Kleinstreuer (2014)]. The

remaining particle passes through the trachea and deposit in the bronchi and alveoli [Tena and Clarà (2012)].

Inhalation and exhalation processes have attracted considerable attention to the researchers in recent years. Investigation the deposition pattern of inhaled particles in the human lung is very challenging due to the complex geometrical structure of the human lung [Kumar et al. (2009); Soni and Aliabadi (2013); Weibel (1963b)]. According to the Weibels's book, most likely in 1731, Rev. Stephen Hales first studied the elasticity of the air in human lung and proposed a dimension for the surface of the human lung [Weibel (1963a)]. The most comprehensive and simple human lung geometry was defined by Weibel's (1963). In case of modelling and simulation of particle transport and deposition in the human lung, Weibel's [Weibel (1963b)] lung model is still being used due to its geometric simplicity. Some geometrical developments of the idealized lung model have been conducted to overcome its complexity [Finlay (2001); Horsfield et al. (1971); Raabe et al. (1976a); Raabe et al. (1976b)]. The most commonly used model for foreign particle movement and detention in the human respiratory tract is that distinguished by a regular and irregular bifurcation pattern [Nowak et al. (2003); Zhang and Kleinstreuer (2004)]. As the Weibel's based human lung geometry model is not realistic. Therefore, in order to obtain the appropriate numerical results for particle transport and deposition, the CFD analysts now focus on realistic airway models [Ma and Lutchen (2006); Ma and Lutchen (2009); Wall and Rabczuk (2008)]. The anatomical based human airway models like Computerized Tomography (CT) scan or Magnetic Resonance Imaging (MRI) geometrical models are becoming more popular in the current literature.

Inhaled particle deposition in the human lung is mainly caused by inertial impaction, Brownian diffusion, gravitational sedimentation and interception [Choi and Kim (2007)]. The airborne particle deposition in human respiratory tract is principally governed by its shape [Hofmann et al. (2009); Kasper (1982)] and size [Hofmann (2011)]. Submicron-particles, which are less than 0.5 μm are initially deposited in the human lung by Brownian diffusion [Hofmann (2011)], while larger particles are deposited by sedimentation and inertial impaction. Breathing pattern is also responsible for particle deposition in human airways. Due to the long residence time slow breathing patterns are more effective for sedimentation and Brownian diffusion, whereas impaction is favoured by fast breathing pattern[Hofmann (2011)]. [Zhang and Kleinstreuer (2002)] have investigated the air flow structure for nanoparticle in the upper airway. They have investigated the turbulent effect on the tracheobronchial area. Cebral and Summers (2004) have investigated the pressure and flow pattern for tracheal and central bronchial in anatomically realistic model and their investigation concluded that decreased pressure and increased shear stress in the stenosis part. Taherian et al. (2011) have performed the unsteady air flow simulation for a CT scan based realistic geometry and have shown the velocity distribution and variation of the vorticity in the lung. Farkas and Szöke (2013), first time created the mucus layer on their non-realistic geometry to simulate the particle deposition. However, they have considered a constant thickness of mucus for all generations which are not physiologically correct. From the above review, most of the above work has been conducted for non-realistic lung geometry. Moreover, none of them investigated the realistic injection properties.

In the present study, we have developed a model for realistic particle transport and deposition in human lungs by creating lung geometry directly from the CT scan

image obtained from an adult healthy patient. We have also applied realistic injection properties to release particles from the inlet and studied the effect of particles' sizes on the deposition.

2. Geometry Generation

In the present study, we have generated the realistic geometry of the human airway. There are several steps to generate the geometry from CT scan or MRI data. First, we have collected the CT image data from a radiologist from a local hospital and the data format is DiCom. The second step is to use AMIRA, the geometry generation commercial software to create the 3D geometry. Then, we have imported the 3D geometry into another software, GEOMAGIC for surface construction. Finally, SOLIDWORKS was used to create the mucus layer inside the geometry.

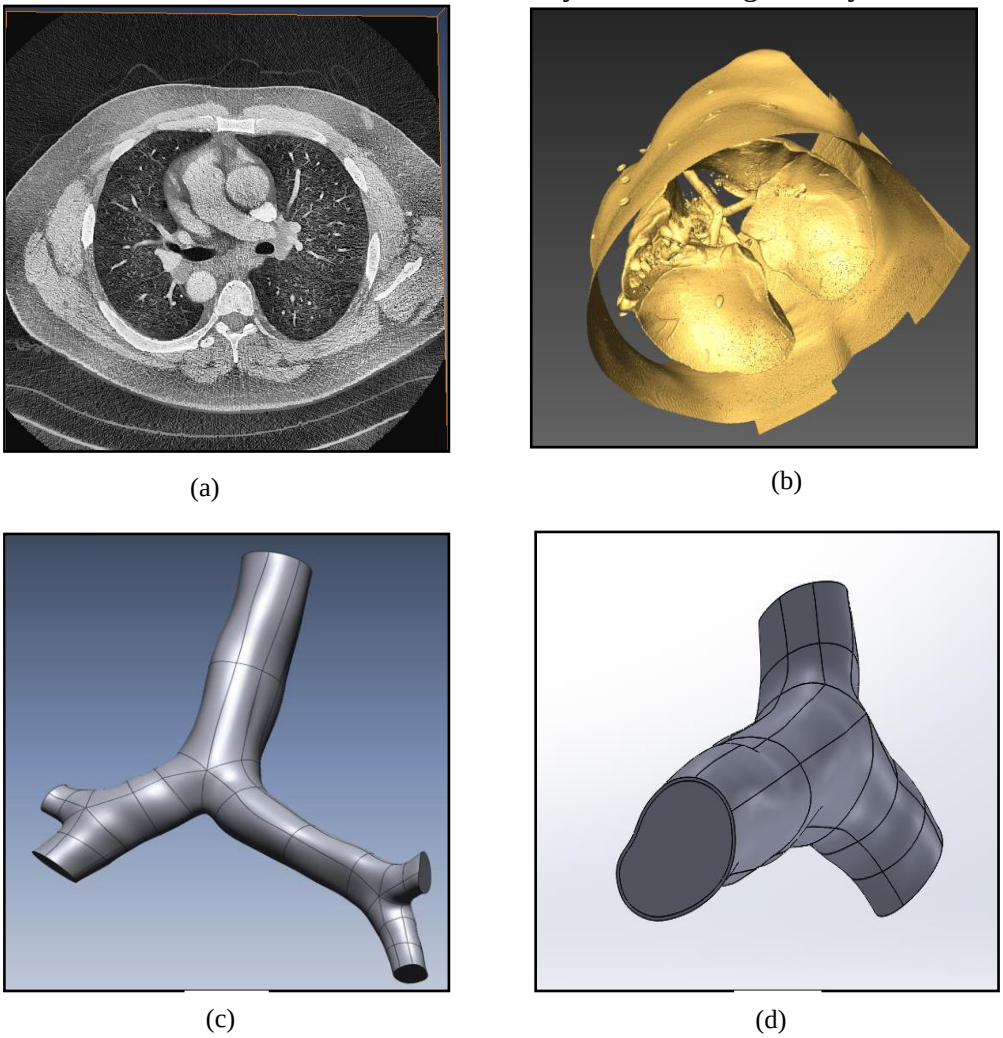

(a) (b)

(c) (d)

Fig. 1(a) CT scan data visualization, (b) Surface rendering and airway visualization, (c) 3D geometry of human lung, and (d) mucus layer of the geometry.

Fig. 1(a) represents the visualization of CT scan data and Fig. 1(b) represents the lung airway geometry after clearing the raw materials from the geometry. Fig. 1(c) represents the 3D human lung geometry and Fig. 1(d) represents the geometry with the mucus layer. As we know the mucus layer thickness varies from generation to generation, thus we have generated a multi-thickness mucus layer on our geometry.

2. Numerical Methods

The complete 3D geometry is imported in ANSYS 15.0 software for simulation purpose. The computational mesh was generated in ANSYS Workbench. A good quality unstructured mesh is generated for the geometry with some inflation layers to correctly capture the boundary layer. Dense mesh has been created on the bifurcation zone where higher velocity gradients are expected. The orthogonal quality of the mesh is calculated as 0.61 above the recommended 0.2 value [put ANSYS manual as reference]. We have generated an unstructured mesh with 1500000 nodes. The grid refinement test is also conducted to obtain the grid independency on numerical solution. The numerical solution of particle transport and deposition are carried out by Lagrangian particle tracking method. We have used the Lagrangian based Discrete Phase Model (DPM), where the air is treated as continuum phase and particle is treated as disperse phase. The continuum phase is governed by the Navier-Stokes equations and the disperse phase can exchange mass, momentum and energy with the continuum phase. In the DPM, the interaction with the continuous phase is considered. We have set the mucus layer properties with the density, 998.2 kg/m^3 and the viscosity, 0.89 *kg/ms*. The pressure-velocity coupling and second order pressure spatial discretization have been used. The residual convergence criteria are set to 10^{-06}. Different injection properties have been used to release the particle from the inlet surface. The boundary conditions used in FLUENT to solve the particle transport and deposition are; the velocity inlet and pressure outlet. The velocity magnitude at inlet is considered as 1 *m/s* and the zero pressure at pressure outlet. A no slip condition is set at the wall. The discrete phase model conditions are used as trap as the boundary condition type. The boundary condition trap means as soon as the particle will touch the wall, it will capture at the wall.

3. Results and Discussion

3.1 Simulation without Mucus Layer

In order to investigate the foreign particle transport and deposition, at first we have simulated the model without any mucus layer inside the geometry. The simulations are carried out for three different particles sizes, $1\mu m$, $5\mu m$ and $10\ \mu m$. The effects of particle size on respiratory deposition have been obtained. According to the physics behind deposition, larger particle should deposit in the upper airway. Fig. 2(a) represents the particle deposition comparison for the three different particles' sizes. One thousand and sixteen particles are released in this simulation and it is observed that in the case of $10\ \mu m$ particles, 428 particles are deposited in the first generation and the rest of the particles have escaped from the simulations. Among the 428 deposited particles, 159 particles are deposited within the first 100 iterations, which represents that most of the particles are deposited in the upper portion of the generation. In case of $5\mu m$ particles, 358 particles are deposited among the 1016 particles, which is less than $10\ \mu m$ particles and the same scenario can be observed for the $1\mu m$ particles.

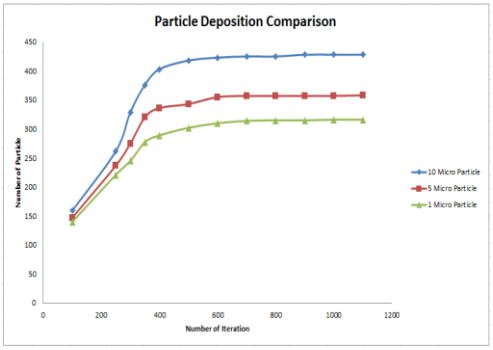

(a)

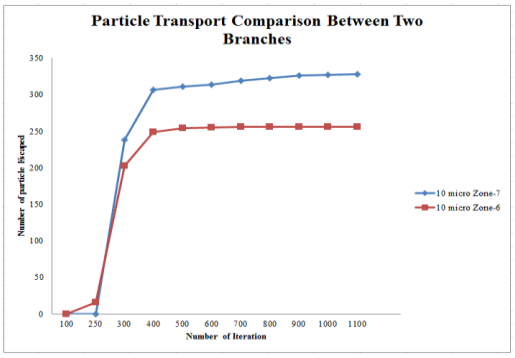

(b)

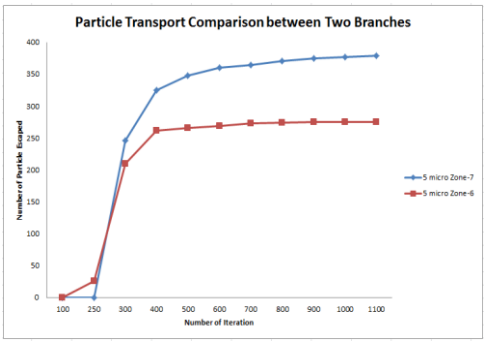

(c)

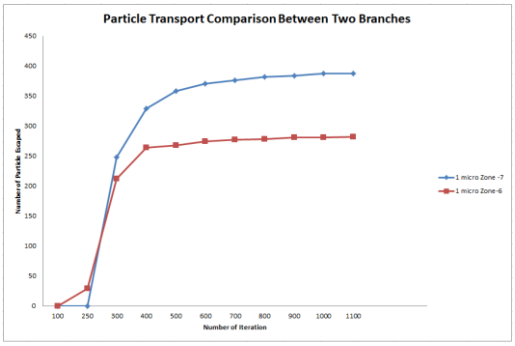

(d)

Fig. 2(a): Particle deposition comparison for different sizes of particles, particle transport comparison for 2(b)$10\ \mu m$, 2(c) $5\ \mu m$ and 2(d)$1\ \mu m$.

Fig. 2(b) represent the particle transport scenario for $10\ \mu m$ particles though the two daughter branches of the first generation. The diameter of the two daughter branches is different and the diameter of the zone 6 is much larger than zone 7. It will be almost 1.5 times larger than zone 7. An interesting scenario is that the branching pattern of the zone 7 is more vertical than zone 6. As the diameter of zone 6 is greater than zone 7, in general, most particles should escape through zone 6. However, realistically most of the particles have escaped through zone 7 despite its lower diameter. The reason for that is that zone 7 is much more vertical compared to zone 6. That is why, larger particle choose this way due to their larger size and inertia. Fig. 2(c) and Fig. 2(d) exhibit the same scenario for particle transport through the two daughter branches.

In order to get a clear idea about the inspiratory deposition pattern, the deposition scenarios for $10\ \mu m$ particle are visualized. Fig. 3(a) represents the particle deposition pattern for $10\ \mu m$ particles. However, for the realistic geometry, we observed that most of the particles are deposited in the wall surface instead of carinal region. It should be noted that the particles have been released by using the inlet surface nodes. The geometrical structure of human lung is not symmetrical and due to its uneven surfaces, the geometrical shape is very complex. On the other hand, non-realistic geometry is symmetrical in shape and it does not have any curve, bends or wave on its wall surface. Moreover, in case of non-realistic geometry, the carinal angle is 45^0. On the other hand, for the realistic geometry, the carinal angle is found to be more than 90^0. As we know, large particle are deposited in the upper portion of the lung airway and inertial impaction is the main mechanism for large particle deposition. In general, all the particles we inhale from the atmosphere follow the air streamline. However, during their movement, when any curve, bends or uneven surface appears

in front of them, they can't follow the air stream due to its large inertia. As a result, those particles are captured by the wall surface.

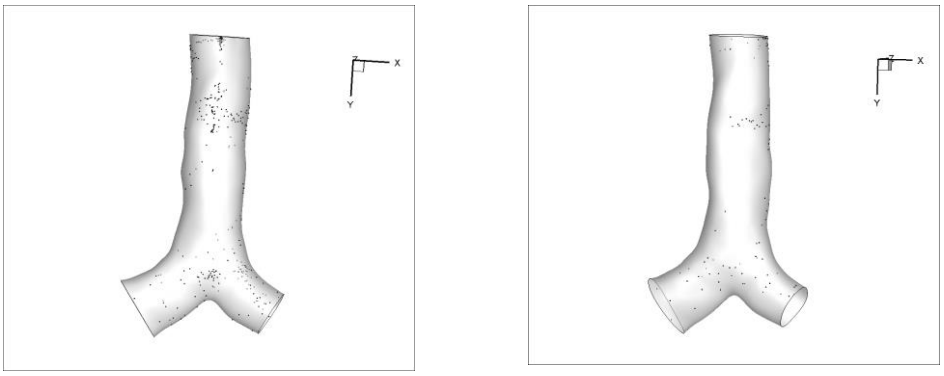

(a) (b)

Fig. 3: Inspiratory deposition pattern of $10\ \mu m$ particles (a) Injection-I (b) Injection-II

Fig. 3 (a) shows that a large number of particles is deposited at the very upper portion of the trachea. Fig. 3 (b) depicts that less particles are deposited at the upper portion of the trachea. Two different injection properties have been used for these two cases and the deposition pattern is different for individual injection. The injection-I and injection-II contains 1016 and 800 particles respectively and the initial positions of the particles are different.

Fig. 4 (a) and Fig. 4 (b) represent the respiratory particle deposition pattern for $5\ \mu m$ particles for different injection. The deposition pattern shows that a large number of particles deposited at the two daughter bronchiole as well the parent bronchiole. We can clearly see that fewer particles are trapped in the right bronchiole compared to $10\ \mu m$ particle. If we compare the two daughter bronchioles, then of course larger particles are deposited at the right bronchiole i.e. zone 7. In case of realistic lung geometry, right branch of the geometry is more vertical than left one. That is why most of the particles have a tendency to go through the right bronchiole. As a result, a large number of particles are deposited at the right bronchiole.

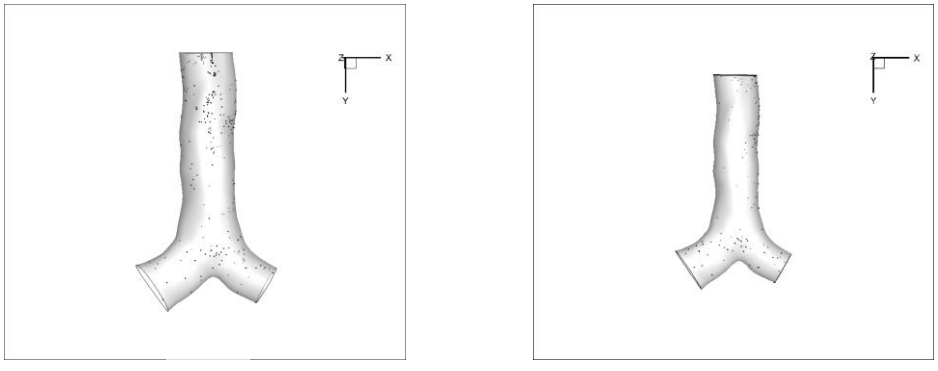

(a) (b)

Fig. 4: Inspiratory deposition pattern of $5\ \mu m$ particles (a) Injection-I (b) Injection-II

The inspiratory particle deposition scenario for $1 \mu m$ particles is shown in Fig. 5(a). From this figure we can clearly observe that very few numbers of particles are deposited at the left bronchiole. The deposition pattern for parent bronchiole is also different compare to larger particle deposition. It is interesting to mention that a good number of particles are deposited in the upper section of the parent bronchiole. Fig.

5(b) depicts the particle deposition pattern for different injection. This figure shows that fewer numbers of particles are deposited at the upper portion.

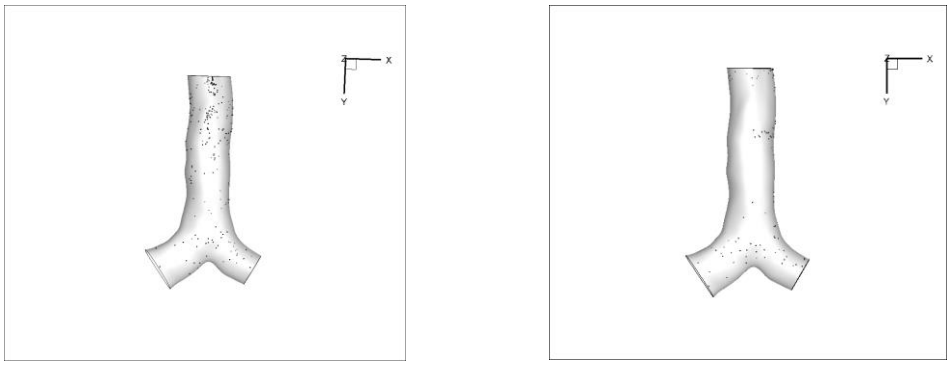

(a) (b)

Fig. 5: Inspiratory deposition pattern of $1\ \mu m$ particles (a) Injection-I (b) Injection-II.

3.2 Simulation with Mucus Layer

We have also investigated the particle transport and deposition for our lung geometry with mucus layer. The particle transport and deposition pattern have been investigated for $10\ \mu m$, $5\ \mu m$ and $1\ \mu m$ particles. We have injected the particles by using the nodes of the inlet surface and the numbers of injected particles are 1054. All appropriate mucus layer properties have been added to simulate the particle transport and deposition. In order to show the deposition pattern, we have collected the trapped particle coordinates on the lung wall. After creating the mucus layer inside the geometry, the diameter of the inlet surface reduces. As a result, the deposition pattern shows a significant difference compared to the case without mucus layer. Fig. 6(a) represents the inspiratory particle deposition pattern for three different sizes of particles. Fig. 6(a) shows that there is a significant difference between the particle depositions for the three different sizes of particles. The graph for $10\ \mu m$ particle shows that a large number of particles is deposited in the first generation compare to two other size particles.

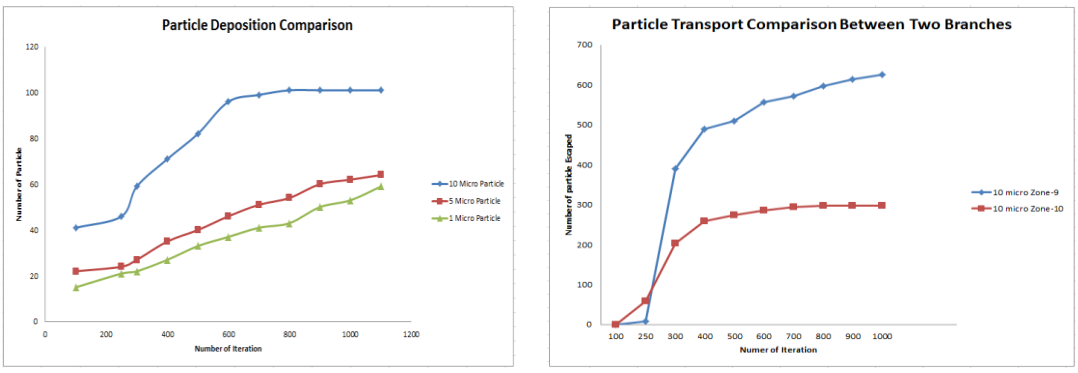

(a) (b)

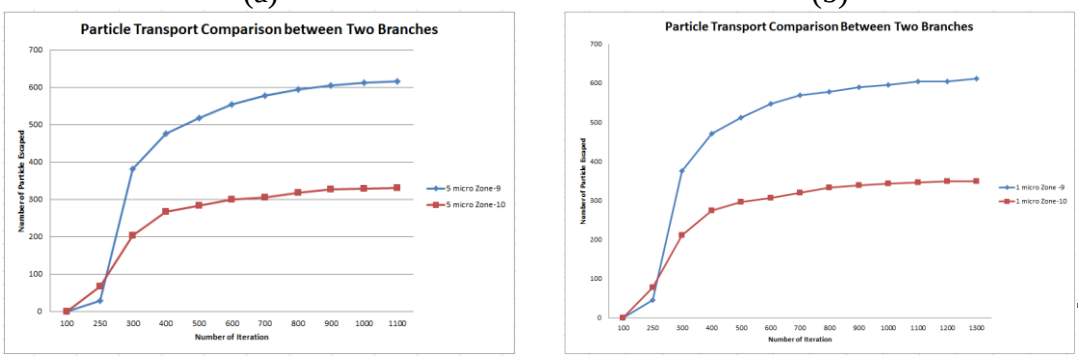

(c) (d)

Fig. 6(a): Particle deposition comparison for different size particle, particle transport comparison for 6(b)$10\ \mu m$, 6(c) $5\ \mu m$ and 6(d) $1\ \mu m$ particle.

Fig. 6(b) represents the particle transport scenario for $10\ \mu m$ particles. From the figure, we can clearly see that a large number of particles are escaping through zone 7. As we explained earlier, two daughter bronchioles are not symmetrical and their diameters are also different. In this case, zone 7 is the smaller daughter bronchioles with small diameter compare to zone 6. In general, due to the large diameter of zone 6, most of the escaped particle should go through the zone 6. But, in this case, most of the particles are escaping through the zone 7 because this bifurcation is more vertical. Fig. 6(c) and Fig. 6(d) represents the particles transport scenario for $5\ \mu m$ and $1\ \mu m$ particle respectively.

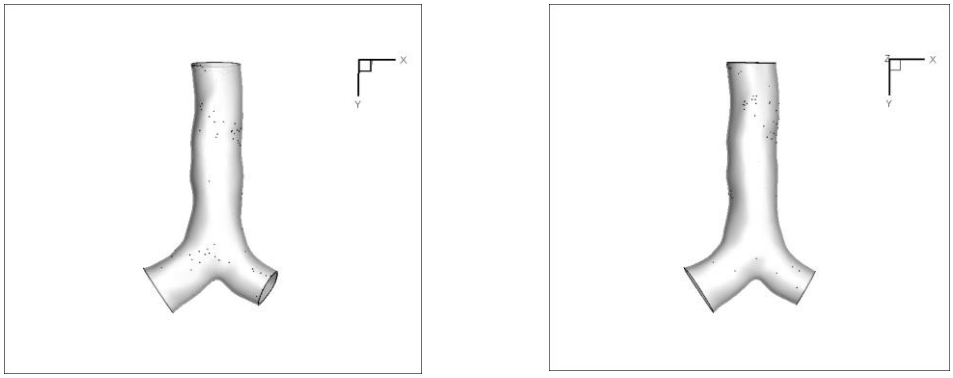

Fig. 7: Inspiratory deposition pattern of $10\ \mu m$ particles (a) Injection-I (b) Injection-II

Fig. 7(a) and Fig. 7(b) represent the respiratory particle deposition scenario for two different injection properties. From the above figure, we can clearly see that the deposition pattern is different for different injection. Fig. 7(a) shows that a good number of particles are deposited at the top of the carinal angle. On contrary, Fig. 7(b) shows that only couple of particles is deposited at the top of the carinal angle.

4. Conclusion

In order to obtain the accurate numerical results of particle transport and deposition in human lung, it is really important to carry out numerical simulations for realistic lung geometry. To investigate the effects of the particle initial position on deposition, different injection techniques have been used and our results suggest that particle deposition is completely dependent on its initial position. The numerical simulations also suggest that the complex geometry of the airway plays an important role in the respiratory deposition. The numerical results also conclude that most of the particles are escaping through the right daughter bronchiole. In order to obtain the effects of mucus layer on deposition, we have carried out the simulation for two cases- with mucus layer and without mucus layer. We have drawn the deposition graph based on number of iterations. The particle deposition comparison graph shows a significant difference between these two cases. The deposition efficiency noticeably increases for $10\ \mu m$ particle in case of mucus layer. The following conclusion can be drawn from the above simulations:

i) The particle deposition pattern is dependent on its initial injection position.

ii) Respiratory geometry plays an important role in case of deposition and the deposition pattern is dependent on lung geometry.
iii) Most of the larger particles have escaped through the right bronchiole in spite of its small diameter.
iv) The deposition efficiency significantly increased for larger particle in case mucus layer.

References

Choi, J.-I. & Kim, C. S. 2007. Mathematical Analysis of Particle Deposition in Human Lungs: An Improved Single Path Transport Model. *Inhalation toxicology,* 19**,** 925-939.

Feng, Y. & Kleinstreuer, C. 2014. Micron-Particle Transport, Interactions and Deposition in Triple Lung-Airway Bifurcations Using a Novel Modeling Approach. *Journal of Aerosol Science,* 71**,** 1-15.

Finlay, W. H. 2001. *The Mechanics of Inhaled Pharmaceutical Aerosols: An Introduction*, Academic Press.

Hofmann, W. 2011. Modelling Inhaled Particle Deposition in the Human Lung—a Review. *Journal of Aerosol Science,* 42**,** 693-724.

Hofmann, W., Morawska, L., Winkler-Heil, R. & Moustafa, M. 2009. Deposition of Combustion Aerosols in the Human Respiratory Tract: Comparison of Theoretical Predictions with Experimental Data Considering Nonspherical Shape. *Inhalation toxicology,* 21**,** 1154-1164.

Horsfield, K., Dart, G., Olson, D. E., Filley, G. F. & Cumming, G. 1971. Models of the Human Bronchial Tree. *Journal of Applied Physiology,* 31**,** 207-217.

Kasper, G. 1982. Dynamics and Measurement of Smokes. I Size Characterization of Nonspherical Particles. *Aerosol Science and Technology,* 1**,** 187-199.

Kumar, H., Tawhai, M. H., Hoffman, E. A. & Lin, C.-L. 2009. The Effects of Geometry on Airflow in the Acinar Region of the Human Lung. *Journal of biomechanics,* 42**,** 1635-1642.

Ma, B. & Lutchen, K. R. 2006. An Anatomically Based Hybrid Computational Model of the Human Lung and Its Application to Low Frequency Oscillatory Mechanics. *Annals of biomedical engineering,* 34**,** 1691-1704.

Ma, B. & Lutchen, K. R. 2009. Cfd Simulation of Aerosol Deposition in an Anatomically Based Human Large–Medium Airway Model. *Annals of biomedical engineering,* 37**,** 271-285.

Nowak, N., Kakade, P. P. & Annapragada, A. V. 2003. Computational Fluid Dynamics Simulation of Airflow and Aerosol Deposition in Human Lungs. *Annals of biomedical engineering,* 31**,** 374-390.

Raabe, O., Yeh, H., Schum, G. & Phalen, R. 1976a. Tracheobronchial Geometry: Human. *Dog, Rat, Hamster*.

Raabe, O. G., Yeh, H.-C., Schum, G. & Phalen, R. F. 1976b. Tracheobronchial Geometry: Human, Dog, Rat, Hamster.

Soni, B. & Aliabadi, S. 2013. Large-Scale Cfd Simulations of Airflow and Particle Deposition in Lung Airway. *Computers & Fluids,* 88**,** 804-812.

Tena, A. & Clarà, P. 2012. Deposition of Inhaled Particles in the Lungs. *Archivos de Bronconeumología (English Edition),* 48**,** 240-246.

Wall, W. A. & Rabczuk, T. 2008. Fluid–Structure Interaction in Lower Airways of Ct-Based Lung Geometries. *International Journal for Numerical Methods in Fluids,* 57**,** 653-675.

Weibel, E. R. 1963a. Chapter I - Introduction. *In:* WEIBEL, E. R. (ed.) *Morphometry of the Human Lung.* Academic Press.

Weibel, E. R. 1963b. Morphometry of the Human Lung.

Zhang, Z. & Kleinstreuer, C. 2004. Airflow Structures and Nano-Particle Deposition in a Human Upper Airway Model. *Journal of computational physics,* 198**,** 178-210.

Zhang, Z. & Kleinstreuer, C. 2002. Transient Airflow Structures and Particle Transport in a Sequentially Branching Lung Airway Model. *Physics of Fluids (1994-present),* 14**,** 862-880.